

PACS numbers: 42.55.Rz; 42.60.Lh
DOI: 10.1070/QE2007v037n08ABEH013610

Diode-pumped solid-state Nd^{3+} : $Ca_3Ga_2Ge_3O_{12}$ crystal lasers

M.I. Belovolov, S.I. Derzhavin, D.A. Mashkovskii, K.S. Sal'nikov,
N.N. Sysoev, M.I. Timoshechkin, A.F. Shatalov

Abstract. **Spectral, luminescent and laser parameters of Nd^{3+} : $Ca_3Ga_2Ge_3O_{12}$ (Nd : CGGG) crystals are studied and compared with the corresponding parameters of Nd : YAG crystals. Continuous-wave spatially single-mode lasing in these crystals at a wavelength of 1.064 μm is investigated upon longitudinal diode pumping through an optical fibre and it is shown that the pump geometries being the same, the output power of a Nd : CGGG laser is close to that of a Nd : YAG laser. The effective cross section σ for induced transitions is measured, which is 1.4×10^{-19} cm^2 for Nd : CGGG crystals. It is found that the 1.064-μm line of the Nd : CGGG laser is inhomogeneously broadened and has a fine structure of four distinct peaks conforming the spectroscopic data about the existence of four main types of activator Nd^{3+} ions in $Ca_3Ga_2Ge_3O_{12}$ crystals. The output power of 700 mW for the absorbed pump power of 2.7 W is obtained for a compact cw solid-state laser with the 1-mm thick active element. It is shown that the thermal distortions of the active element are the main mechanisms limiting the output power of a solid-state Nd : CGGG crystal laser.**

Keywords: *solid-state lasers, diode pumping, laser crystals.*

1. Introduction

Neodymium-doped calcium – gallium – germanium – garnet Nd^{3+} : $Ca_3Ga_2Ge_3O_{12}$ (Nd : CGGG) crystals are promising materials for fabricating compact and low-cost diode-pumped solid-state lasers because these crystals can be doped with large concentrations of Nd^{3+} ions and combine attractive spectral and luminescent as well as physical and technological properties [1 – 3]. The Nd : CGGG crystals belong to disordered media and have inhomogeneously broadened absorption and luminescence spectra of Nd^{3+} ions. This broadening facilitates the matching of the absorption spectra of the laser crystal with the emission spectra of laser diode pump sources and makes this crystal promising for generating short laser pulses and for fabricating tunable lasers [4]. The CGGG crystal has a cubic symmetry and, hence, is optically isotropic. The thermal conductivity of this crystal is nearly as large as that of widely used YAG crystals and substantially exceeds the thermal conductivity of laser glasses. The crystals of a high optical quality with the atomic concentration of neodymium of about 30 % can be grown in air at a high speed in platinum crucibles. The main physical and technological parameters of Nd : CGGG and Nd : YAG crystals borrowed from papers [2, 3, 5, 6] and presented in Table 1 illustrate the above-mentioned advantages of Nd : CGGG crystals.

The use of Nd : CGGG crystals for fabricating solid-state diode-pumped lasers was first reported in 1996 [5]. The output power of 150 mW was achieved. Later, spectral and luminescent parameters of the concentration series of Nd : CGGG crystals was studied and the output power of up to 300 mW was obtained in the multimode regime in crystals with the atomic concentration of Nd^{3+} ions of about 2 % [7, 8].

The efficiency of solid-state lasers mainly depends on the type and output power of the pump source, the selected excitation scheme and matching conditions of the pump source with the active element of the laser, on the quality and size of the active element, concentration of activator ions, etc. Therefore, to obtain reliable data on the lasing parameters on a new active element, measurements should be performed under the same geometrical conditions of the experiment; the absolute values of parameters should be measured simultaneously on a reference laser element made of a known and well-studied laser material for the following comparison of their efficiencies.

The aim of this paper is to study compact solid-sate higher-power Nd : CGGG crystal lasers and to compare spectral, luminescent and lasing parameters of Nd : CGGG crystals with the corresponding parameters of Nd : YAG crystals upon longitudinal diode pumping through the optical fibre.

2. Absorption and luminescence spectra and radiation lifetimes

Spectral, luminescent and lasing parameters were measured in Nd : YAG crystals with the 2×10^{20}-cm^{-3} concentration

M.I. Belovolov, K.S. Sal'nikov, A.F. Shatalov Fibre Optic Research Center, Russian Academy of Sciences, ul. Vavilova 38, 119333 Moscow, Russia; e-mail: shatalov@fo.gpi.ru;
S.I. Derzhavin, D.A. Mashkovskii A.M. Prokhorov General Physics Institute, Russian Academy of Sciences, ul. Vavilova 38, 119991 Moscow, Russia;
N.N. Sysoev Department of Physics, M.V. Lomonosov Moscow State University, Vorob'evy gory, 119992 Moscow, Russia;
M.I. Timoshechkin Laser Materials and Technology Research Center, A.M. Prokhorov General Physics Institute, Russian Academy of Sciences, ul. Vavilova 38, 119991 Moscow, Russia

Received 27 April 2007; revision received 15 June 2007
Kvantovaya Elektronika **37** (8) 753 – 759 (2007)
Translated by I.A. Ulitkin

Table 1. Physical and technological parameters of Nd : YAG and Nd : CGGG laser crystals.

Laser crystal	Parameters						
	Admissible atomic concentrations of Nd^{3+} ions (%)	Thermal conductivity/W (m °C)$^{-1}$	Melting temperature/°C	Crucible material	Growth method	Atmosphere	Growth rate/mm h^{-1}
Nd : YAG	$\leqslant 1$	12 – 14	1970	Ir	Czochralski	Ar, N_2	~0.5
Nd : CGGG	$\leqslant 30$	10.9	~1400	Pt	Czochralski	Air	~2

of Nd^{3+} ions. Crystals were grown by the Czochralski method in the oxidising atmosphere. The laser elements were cut from the crystal in the form of rectangular plates of size 5×5 mm and thickness $d = 1$ and 1.5 mm. As a laser material to be compared with, we chose Nd : YAG with the radiative lifetime $\tau \approx 230$ μs, which is close to τ for Nd : CGGG, and with the 0.8×10^{20}-cm^{-3} concentration of Nd^{3+} ions. The laser element made of Nd : YAG represented a disk of diameter 10 mm and thickness $d = 4.1$ mm. The output facets of laser elements had dielectric mirror coatings with the transmission coefficient of more than 95 % at the pump wavelength ($\lambda_p \approx 0.8$ μm) which completely reflected radiation ($R \geqslant 99$ %) at the lasing wavelength ($\lambda_g = 1.06$ μm). The other facets of laser elements had AR coatings for these wavelengths. The laser elements were used in laser resonators with the external (spherical or plane) output mirrors.

The absorption spectra were measured by transmitting the radiation from a white light source (halogen lamp) through a sample and coupling it into a multimode optical fibre with the numerical aperture NA = 0.22 and the core diameter $d_c = 100$ μm, which was connected to the fibre input of an MS96A spectrum analyser (Anritsu). The spectral range of the spectrum analyser was from 0.6 to 1.6 μm, the spectral resolution was 0.1 nm and the measurement accuracy of the absolute value of the wavelength was ~ 0.1 nm.

Figure 1 shows the absorption spectra of the Nd : YAG ($d = 4.1$ mm) and Nd : CGGG ($d = 1.5$ mm) crystals in the wavelength region from 0.78 to 0.82 μm, which were recorded with the resolution of 0.5 nm. One can see that the laser elements made of Nd : CGGG have broader absorption bands than analogous absorption bands in Nd : YAG crystals, which is caused by the multi-centre structure of the Nd : CGGG crystal. The most intense absorption bands in Nd : YAG and Nd : CGGG are located at 0.8085 and 0.805 μm, respectively. The FWHM of these bands is 0.7 nm for Nd : YAG and ~ 2.7 nm for Nd : CGGG, i.e. the absorption bands for selective pumping in laser elements made of Nd : CGGG are four times broader. Therefore, the absorption spectrum of Nd : CGGG matches better with the emission spectrum of semiconductor pump lasers, whose characteristic emission bandwidth is 1–3 nm and this matching is more stable upon temperature variations. These properties of the pump system for Nd : CGGG crystals is an important advantage of diode-pumped lasers. In addition, the absorption coefficient at the maximum of the most intense absorption band of Nd : CGGG is 11 cm^{-1}, and that of Nd : YAG is 5 cm^{-1}. Thus, although the thickness of the Nd : CGGG laser element is 2.7 times smaller than that of the Nd : YAG laser element, the absorption efficiency of pump radiation at the maximum of absorption of these crystals was approximately the same and was ~ 70 %.

To measure the luminescence spectra, the radiation from the pump source was focused into a spot at the sample edge.

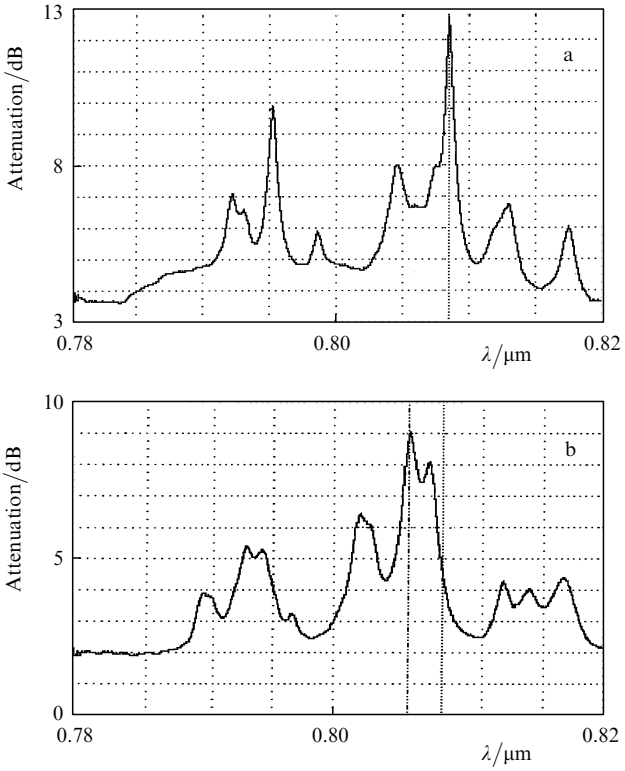

Figure 1. Absorption spectra of Nd : YAG (a) and Nd : CGGG (b) crystal laser elements.

The luminescence emission was collected by a microobjective in the direction perpendicular to the pump radiation propagation and was coupled into the fibre (NA = 0.22, $d_c = 100$ μm) whose output end was connected to the spectrum analyser. Luminescence was excited at 0.8 μm by a semiconductor AlGaAs heterostructure laser diode operating in the cw and pulsed regimes with the peak power of up to 0.5 W. During the experiments, the laser diode was kept at a constant temperature of about 20 °C with the accuracy of ~ 0.1°C with the help of a temperature stabilisation scheme based on Peltier elements. Its lasing wavelength at room temperature was ~ 0.805 μm and the emission bandwidth was 1.0 nm. The pump wavelength was tuned to the absorption line of the laser crystal by changing the laser diode temperature.

Figure 2 shows the luminescence spectra of Nd : CGGG and Nd : YAG crystals in the region of 1.06 μm. The main luminescence bands of the Nd : YAG crystal are located at 1.0517, 1.0611, 1.0637, 1.0675, 1.0734 and 1.0775 μm, which agrees with the known transition wavelengths between the sublevels of the $^4F_{3/2}$ and $^4I_{11/2}$ terms of the Nd^{3+} ion in a YAG crystal [6]. The wavelength of the most intense luminescence band is 1.0637 μm and its FWHM is ~ 1 nm. We studied lasing at this wavelength.

The luminescence bands of the Nd : CGGG crystal in the region from 1.05 to 1.09 μm are located at 1.0595,

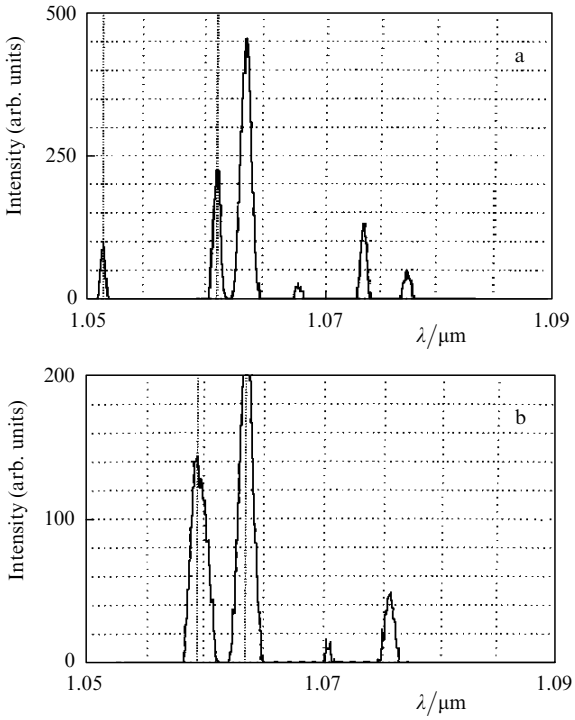

Figure 2. Luminescence spectra of Nd : YAG (a) and Nd : CGGG (b) crystals in the 1.06-μm region.

1.0635, 1.0704 and 1.0755 μm, which agrees with the spectroscopic data obtained in [3]. Lasing in the Nd : CGGG crystal was obtained at the most intense 1.064-μm luminescence band. The FWHM of this band is ~ 1.5 nm, which is 1.5 times higher than that for the Nd : YAG crystal.

To measure the luminescence kinetics, rectangular 80-μs current pulses with the pulse period of 6 ms and steep front of ~ 1 μs were fed to the pump laser diode. The duration and the repetition rate of current pulses from the power supply of the laser were selected taking into account the characteristic luminescence time of neodymium garnets, which is 200 – 260 μs.

In the reference Nd : YAG sample, the measured lifetime τ^{YAG} of the upper $^4F_{3/2}$ laser level was 230 μs, which agrees within the measurement error ($\sim 10\,\%$) with data [9]. In the Nd : CGGG sample under study, the lifetime τ^{CGGG} of this level was 220 μs. It represents a value averaged over the activator centres N, L, X and Y [3] with the close lifetimes (~ 200 μs).

Table 2 presents the measured spectral and luminescent parameters of Nd : CGGG and Nd : YAG crystals. The concentration of Nd^{3+} ions in the Nd : CGGG samples was ~ 2.4 times higher that that in the Nd : YAG sample and, hence, the absorption efficiency of pump radiation by this crystal at $\lambda \approx 0.805$ μm is considerably higher than in Nd : YAG crystals. In this case, the radiation lifetimes, which characterise the intensity of processes of concentration quenching, are virtually the same in the samples under study. The presented spectral and luminescent parameters of Nd : CGGG and Nd : YAG crystals and concentrations of Nd^{3+} ions indicate that the laser elements made of these crystals (of thickness 1.5 and 4.1 mm, respectively) absorb approximately the same pump power, and the lasing power can be used to compare the efficiency of Nd : CGGG and Nd : YAG laser materials and Nd^{3+} ions as working ions in these crystals.

3. Lasing parameters upon diode pumping through the optical fibre and effective cross section for stimulated emission at the $^4F_{3/2} \rightarrow {}^4I_{11/2}$ transition

Figure 3 shows the scheme of the experimental setup for obtaining lasing on laser crystals upon longitudinal diode pumping through the optical fibre. An HLU32F400-808 LIMO laser-diode array with the fibre output (NA = 0.22, $d_c = 400$ μm) was used as a pump source. The maximum output power of the array was 30 W, $\lambda_p = 808$ nm, the FWHM $\Delta\lambda$ of the emission band was ~ 3 nm. To improve the conditions of spatial matching of pump radiation with the fundamental mode of the resonator (for our resonator the waist-beam diameter was $2\omega_0 = 184$ nm) and simplify the obtainment of spatial single-mode (the TEM_{00} mode) lasing, the radiation of laser-diode array (*1*) through fibre output (*2*) was coupled by a system of lenses (*3*) into optical fibre (*4*) with a smaller core diameter $d_c = 2\omega_{0p} =$ 100 μm and the same numerical aperture NA = 0.22. The end of optical fibre (*4*) was tightly attached perpendicular to the front facet (shown in Fig. 3 by a black rectangle) of laser element (*5*), which was fixed on the copper heatsink with a thermal paste. The front facet – the output mirror of

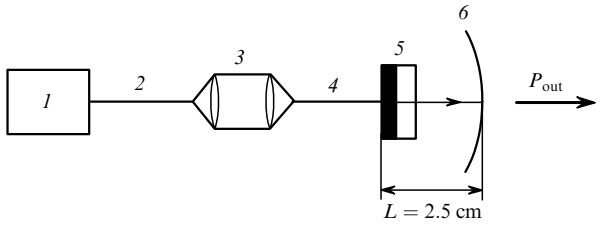

Figure 3. Scheme of the experimental setup: (*1*) laser-diode array; (*2*) optical fibre of the laser diode pump system ($d_c = 400$ μm, NA = 0.22); (*3*) collimating and focusing lenses ($f = 30$ mm, NA = 0.22); (*4*) optical fibre for exciting single mode lasing ($d_c = 100$ μm, NA = 0.22); (*5*) laser element; (*6*) output spherical mirror with the radius of curvature of 5 cm.

Table 2. Spectral and luminescent parameters of Nd : YAG and Nd : CGGG crystals.

Laser crystal	Parameters					
	Absorption band wavelength/nm	Peak absorption coefficient/cm^{-1}	Absorption band FWHM/nm	Luminescence peak wavelength/nm	Luminescence peak FWHM/nm	τ/μs
Nd : YAG	808.5	5	0.7	1063.7	1	230
Nd : CGGG	805	12	2.3	1063.5	1.5	220

Note: Concentrations of Nd^{3+} ions are 0.8×10^{20} and 2×10^{20} cm^{-3} for Nd : YAG and Nd : CGGG, respectively.

the laser element – together with spherical mirror (*6*) with the transmission coefficient $T = 0.011$ form a semiconfocal resonator of length $L = 2.5$ cm.

By using this experimental setup, we obtained and studied the spatially single-mode cw lasing in Nd : CGGG ($d = 1.5$ mm) and Nd : YAG ($d = 4.1$ mm) crystals at room temperature. Figure 4 shows the dependences of the output power P_{out} of the Nd : YAG and Nd : CGGG crystal lasers on the absorbed pump power P_a. For the Nd : YAG laser, the threshold absorbed pump power P_{th}^{YAG} was 31 mW, the slope efficiency η^{YAG} was 0.27, while for the Nd : CGGG laser, $P_{th}^{CGGG} = 39$ mW and $\eta^{CGGG} = 0.22$. It follows from Fig. 4 that the lasing thresholds in Nd : CGGG crystals as low as that in typical Nd : YAG crystals are achieved. Absolute values of the lasing power in Nd : CGGG crystals were 20 % – 30 % lower than those in Nd : YAG crystals, which indicates a rather high lasing efficiency of Nd^{3+} ions in the CGGG crystal lattice. The output power of the Nd : CGGG laser depends to a lesser degree on the temperature variations of the pump laser diode, which is explained by broader absorption spectra of this crystal and represents one of its advantages compared to the Nd : YAG crystal.

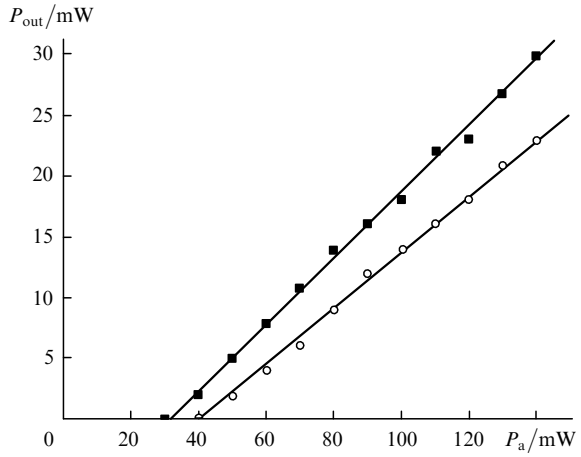

Figure 4. Dependences of the output power of spatially single-mode lasing of solid-state Nd : YAG (■) and Nd : CGGG (○) lasers on the absorbed power upon diode pumping through the optical fibre ($d_c = 100$ μm, NA = 0.22).

For the four-level lasing scheme on Nd^{3+} ions, the effective cross section for the stimulated emission at the $^4F_{3/2} \rightarrow {}^4I_{11/2}$ transition, obtained by taking into account different activator centres and transitions between Stark sublevels, is determined by the expression [10]

$$\sigma = \frac{h\nu_p}{2\tau}\frac{\lambda_p}{\lambda_g}\frac{T}{P_{th}\eta}S_{eff}, \tag{1}$$

where $h\nu_p$ is the pump-photon energy and S_{eff} is the effective mode 'area', which takes into account the overlap of the pump beam and the fundamental resonator mode.

The expression for the effective mode area has the form [11]

$$S_{eff} = \left(d\int_V p(r,z)s(r,z)\mathrm{d}V\right)^{-1}, \tag{2}$$

where $p(r,z)$ and $s(r,z)$ are normalised distributions of the pump power and the fundamental resonator mode; and V is the pumped volume of the crystal. In our experiments we used a laser-diode array with a fibre output. The optical fibre was tightly attached to the crystal so that the symmetry axis of the fibre coincides with the optical axis of the resonator. The radius ω_p of the pump beam at the output of the multimode fibre can be approximately determined by the expression [11]

$$\omega_p^2 = \omega_{p0}^2\left[1 + \left(\frac{\lambda_p M_p^2 z}{n\pi\omega_{p0}^2}\right)^2\right], \tag{3}$$

where ω_{p0} is the radius of the fibre core; M_p^2 is the parameter of the beam quality; n is the refractive index of the crystal; z is the distance from the fibre end to the cross-section plane of the pump beam in which the beam radius is ω_p. The corresponding normalised distribution function of the pump power within the crystal has the form (see [11, 12])

$$p(r,z) = \frac{\alpha \mathrm{e}^{-\alpha z}}{\pi\omega_p^2(1-\mathrm{e}^{-\alpha d})}\Theta(\omega_p^2 - r^2), \tag{4}$$

where α is the absorption coefficient of the crystal sample; and $\Theta(x)$ is the Heaviside function. The normalisation condition is written in the form

$$\int_V p(r,z)\mathrm{d}V = 1. \tag{5}$$

Then, the normalised power distribution of the fundamental TEM_{00} mode is

$$s(r,z) = \frac{2}{\pi\omega_0^2 d}\exp\left(-\frac{2r^2}{\omega_0^2}\right). \tag{6}$$

The overlap of the fundamental mode of the resonator and the pump beam is schematically shown in Fig. 5. The values of S_{eff} calculated by (2)–(6) for lasers with active Nd : CGGG and Nd : YAG elements were 2.6×10^{-4} cm^2 and 6.0×10^{-4} cm^2, respectively. By using (1), the obtained

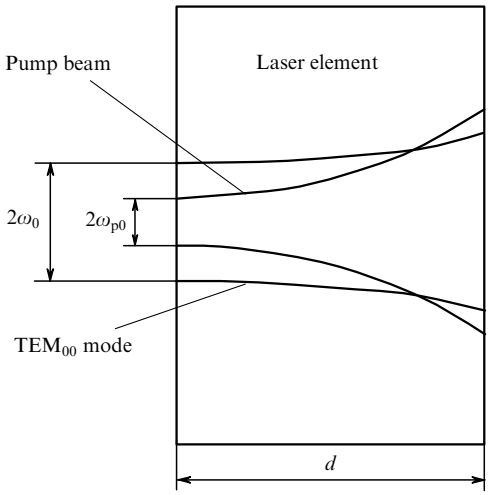

Figure 5. Scheme of matching the pump field and the mode field of the resonator for calculating the effective area of the generated mode of a solid-state laser diode pumped through a fibre system.

Table 3. Lasing parameters of Nd : YAG and Nd : CGGG crystals upon longitudinal diode pumping through the fibre system.

Laser crystal	Parameters					
	P_{th}/mW	η	Resonator losses (%)	Averaged effective cross section for the induced $^4F_{3/2} \rightarrow {}^4I_{11/2}$ transition/10^{-19} cm^2	λ_g/μm	Emission spectrum FWHM/nm
Nd : YAG	31	0.27	2	3.2	1.064	0.3
Nd : CGGG	39	0.22	3	1.4	1.064	0.6

Note: Concentration of Nd^{3+} ions in crystals is as that in Table 2.

experimental data ($P_{th}^{YAG} = 31$ mW, $\eta^{YAG} = 0.27$, $P_{th}^{CGGG} = 39$ mW, $\eta^{CGGG} = 0.22$, $\tau^{YAG} = 230$ μs, $\tau^{CGGG} = 220$ μs, $\lambda_g \approx 1.06$ μm, $\lambda_p \approx 0.8$ μm, $M_p = 40$), the calculated values of S_{eff} and the transmission coefficient of the output mirror $T = 0.01$, we determined the effective cross sections for induced $^4F_{3/2} \rightarrow {}^4I_{11/2}$ transitions for our samples: $\sigma_{CGGG} = 1.4 \times 10^{-19}$ cm^2 and $\sigma_{YAG} = 3.2 \times 10^{-19}$ cm^2. The obtained effective absorption cross section for the induced transition σ_{YAG} for the Nd : YAG crystal agrees with the values presented in [10, 13] and confirms the reliability of the obtained value of the effective cross section for the Nd : CGGG crystal.

It follows from the obtained data on absolute values of the lasing power and cross sections for induced transitions that Nd^{3+} ions in the CGGG crystal operate during lasing with a lower efficiency than in YAG crystals. The reason of this is, obviously, the peculiarities of a more complex CGGG crystal, where Nd^{3+} ions can enter the lattice in different positions, which is confirmed by spectroscopic studies [3].

Figure 6 shows the emission spectra of the Nd : YAG and Nd : CGGG lasers at 1.06 μm. The wavelength, at which the maximum output power of the Nd : YAG laser was observed, was 1.0637 μm and the FWHM of the emission line was ~ 0.3 nm. This lasing line corresponds to the $^4F_{3/2} \rightarrow {}^4I_{11/2}$ transition between the energy sublevels of the Nd^{3+} ion in the YAG crystal [6].

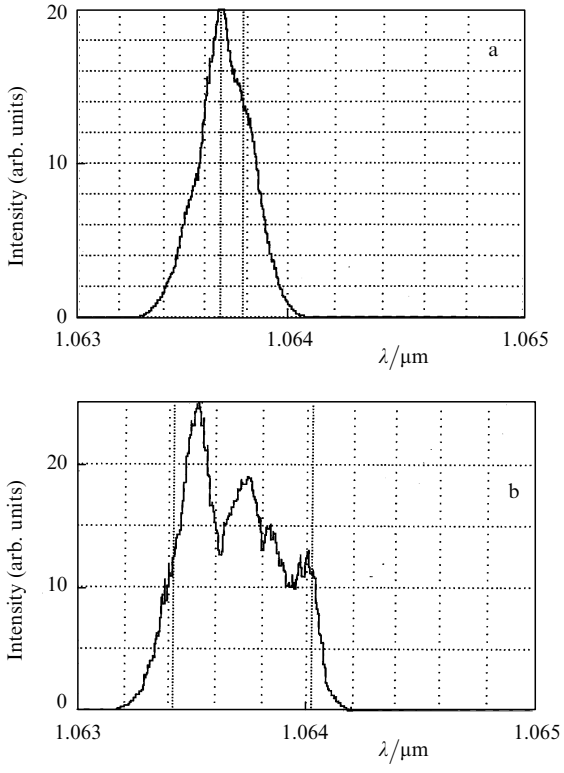

Figure 6. Spatially single-mode emission spectra of solid-state Nd : YAG (a) and Nd : CGGG (b) lasers at 1.06 μm.

The maximum output power of the Nd : CGGG laser was achieved at 1.0637 μm and the FWHM of the lasing line was 0.6 nm. The lasing line of this laser, compared to the Nd : YAG laser, has a distinct fine structure consisting of four peaks, which agrees with the presence of several types of activator centres in Nd^{3+} ions in CGGG [3]. The lasing wavelengths, at which these peaks were observed, were 1.0635, 1.0637, 1.0638 and 1.0640 μm. One can see from Fig. 6 that the lasing lines of the Nd : CGGG laser have different intensities and two lines (the shortest wavelength and the longest wavelength) differ in intensity almost by two. A comparatively wide lasing line (~ 0.6 nm) makes it possible to use the Nd : CGGG crystal for tunable lasing, optical heterodyning and for emitting short laser pulses. The lasing parameters of Nd : YAG and Nd : CGGG crystals measured in this paper are presented in Table 3. The obtained data indicate that the lasing characteristics of Nd : CGGG are close to the characteristics of Nd : YAG crystals and have significant advantages related to their more thermally stable pump scheme and compactness of laser elements.

4. Output parameters of the Nd : CGGG laser at high pump powers

In experiments aimed at studying the lasing parameters at high pump powers, the resonator length was reduced in our setup (see Fig. 3) to the minimum possible value ($L = 1.5$ cm) and lenses (*3*) and fibre (*4*) were replaced by a microobjective, which focused pump radiation from fibre end (*2*) directly on the crystal into a spot of size ~ 400 μm. A decrease in the resonator length and an increase in the pump-beam cross section weakened the effect of the thermal lens on lasing, which allowed us to achieve the maximum output power from the solid-state laser for the selected parameter of the laser setup. To study the dependence of the lasing efficiency on the thickness of the laser element, we additionally manufactured a 1-mm thick sample from the Nd : CGGG crystal, which was analogous in its properties to the 1.5-mm thick sample. 60 % and 80 % of pump radiation was absorbed per round trip in these laser elements, respectively.

Figure 7 presents experimental dependences of the output power of the Nd : CGGG laser on the absorbed pump power. One can see that when the absorbed power exceeds the threshold value $P_{th} = 130$ mW, the output power of the laser with the 1-mm thick laser element first grows linearly with the slope efficiency $\eta = 0.3$ up to $P_{out} = 560$ mW,

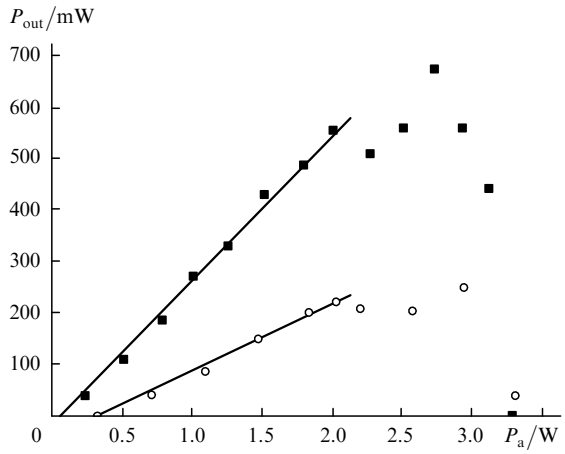

Figure 7. Dependences of the output power of multimode lasing of compact solid-state Nd : CGGG lasers on the absorbed pump power for 1-mm thick (■) and 1.5-mm thick (○) laser elements.

which corresponds to the absorbed pump power $P_a = 2$ W. For $P_a > 2$ W, deviations from the linear dependence appear. The output power achieves its maximum value $P_{out}^{max} \approx 700$ mW for $P_a = 2.7$ W and then drastically vanishes.

The dependence of the output power on the absorbed pump power for a solid-state laser with the 1.5-mm thick laser element is qualitatively the same as in the case of the 1-mm thick laser element, however the lasing power is lower. The threshold absorbed power P_{th} for this laser was 390 mW and the slope efficiency η on the linear part was 0.14. The deviation from the linear dependence was observed for the same absorbed pump power $P_a = 2$ W as in the solid-state laser with the 1-mm thick laser element, but the output power was much lower ($P_{out} = 220$ mW). The maximum output power P_{out}^{max} was $\sim$250 mW for $P_a = 2.9$ W. Lasing in both samples terminated at $P_a = 3.3$ W and the laser element was damaged at $P_a \approx 4$ Вт.

The deviation of the obtained dependence from the linear law is caused by the thermal distortions of resonators of the solid-state laser [14], which lead to the appearance of an induced thermal lens in the laser element. In our case, such a laser element can be treated as a mirror with a radius of curvature equal to the focal length of the thermal lens [15]. As the pump power increases, the radius of curvature decreases. When it is smaller than the resonator length, the system becomes unstable and lasing is quenched. At smaller resonator lengths, the quenching should occur at high absorbed pump powers, which was observed in the experiment. The optical power of the thermal lens, determining the characteristic properties of the dependence of the output power on the absorbed pump power, is proportional to the pump power density [16], which is equal to the pump power divided by the pump-beam cross section. Because the pump geometry remained the same, the dependences of the output power on the absorbed pump power for elements of different thickness look qualitatively similar. The lasing efficiency of a solid-state laser with a thicker laser element was lower because nonactive losses increase with increasing the thickness of the laser element and conditions of the spatial matching of the pump radiation and fundamental resonator modes deteriorate.

It follows from the obtained experimental data that high output powers and optical efficiencies are possible to achieve by selecting optimal parameters of the resonator and laser elements.

5. Conclusions

We have compared spectral, luminescent and lasing parameters of Nd : YAG and Nd : CGGG crystals. It has been shown that the absorption and luminescence spectra of Nd^{3+} ions in Nd : CGGG crystals are broader, which is explained by the multicentre structure of CGGG. This facilitates the matching of the pump spectra of laser diodes with the excitation spectra of Nd : CGGG crystals and provides higher lasing stability upon varying the external temperature.

We have studied the lasing parameters of spatially single-mode Nd : CGGG crystal lasers with the 2×10^{20}-cm^{-3} concentration of Nd^{3+} ions upon diode pumping through the optical fibre, and compared them with the analogous parameters of known laser Nd : YAG crystals with the 0.8×10^{20}-cm^{-3} concentration of Nd^{3+} ions. The effective cross section of induced transitions $\sigma_{CGGG} = 1.4 \times 10^{-19}$ cm^2 has been determined for the Nd : CGGG crystals, which is averaged over four main lines observed in the emission spectrum.

We have shown that Nd : CGGG laser crystals under study are close in efficiency to Nd : YAG laser crystals and have a number advantages caused by a greater bandwidth of the pump-radiation absorption (by approximately three times), high efficiency of the pump absorption and a simpler manufacturing technology and lower cost of these garnets. It has been found that the emission spectrum of the 1.064-μm Nd : CGGG laser is inhomogeneously broadened and consists of four distinct peaks, which confirm the spectroscopic data about the existence of several (at least, four) activator centres for the Nd^{3+} ions in $Ca_3Ga_2Ge_3O_{12}$ crystals.

Lasing parameters of a compact Nd : CGGG crystal laser at high pump powers have been determined and it has been shown that in this case the increase in the output power is limited by the appearance of a thermal lens. The output power of 700 mW has been achieved in the cw regime for the absorbed pump power of 2.7 W.

Our study has shown that Nd : CGGG is a promising laser crystal for fabricating compact, efficient and low-cost lasers operating in a wide range of output powers. The inhomogeneously broadened emission spectrum of the Nd : CGGG laser is of interest for obtaining tunable lasing, optical heterodyning as well as optical amplification and generating short laser pulses.

References

1. Es'kov N.A., Osiko V.V., Sobol' A.A., Timoshechkin M.I., Butaeva T.I., Ngok Chan, Kaminsky A.A. *Neorgan. Material.*, **14**, 2254 (1978).
2. Petrunin G.I., Popov V.G., Timoshechkin M.I. *Fiz. Tverd. Tela*, **309**, 139 (1989).
3. Voron'ko Yu.K., Kabachenko V.Ya., Krysanova L.I., Osiko V.V., Sobol' A.A., Timoshechkin M.I. *Neorgan. Material.*, **19**, 959 (1983).
4. Shatalov A.F., Timoshechkin M.I., Belovolov M.I., Gladyshev A.V. *Tez. dokl. Vseross. nauchn. konf. 'Lazery. Izmereniya. Informatsiya'* (Proc. All-Russian Sci. Conf. on

'Lasers. Measurements. Information') (St. Petersburg, 2003) p. 88.
5. Belovolov M.I., Dianov E.M., Timoschechkin M.I., Morosov N.P., Prokhorov A.M., Timoschechkin K.M. *Proc. CLEO/Europe'96* (Hamburg, Germany, 1996) Paper CThI60, p. 281.
6. Zverev G.M., Golyaev Yu.D. *Lazery na kristallakh i ikh primenenie* (Crystal Lasers and Their Application) (Moscow: Radio i svyaz', 1988).
7. Jaque D., Caldino U., Romero J.J., Garcia Sole J. *J. Appl. Phys.*, **86**, 6627 (1999).
8. Jaque D., Romero J.J., Garcia Sole J. *J. Appl. Phys.*, **92**, 3436 (2002).
9. Basiev T.T., Dianov E.M., Prokhorov A.M., Shcherbakov I.A. *Dokl. Akad. Nauk USSR*, **216**, 297 (1974).
10. Naito K., Yokotani A., Sasaki T., Okuyama T., Yamanaka M., Nakatsuka M., Nakai S., Fukuda T., Timoschechkin M.I. *Appl. Opt.*, **32**, 7387 (1993).
11. Chen Y.-F. *J. Appl. Phys. B*, **70**, 475 (2000).
12. Romero J.J., Jaque D., et al. *J. Appl. Phys.*, **92**, 1754 (2002).
13. Mermilliod N., Romero R., Chartier I., Garapon C., Moncorge R. *IEEE J. Quantum Electron.*, **28**, 1179 (1992).
14. Dianov E.M., Prokhorov A.M. *Dokl. Akad. Nauk USSR*, **192**, 531 (1970).
15. Vedyashkin N.V., Derzhavin S.I., Kuz'minov V.V., Mashkovskii D.A. *Kvantovaya Elektron.*, **33**, 367 (2003) [*Quantum Electron.*, **33**, 367 (2003)].
16. Mukhopadhyay P.K., Ranganathan K., Jogy J., Sharma S.K., Nathan T.P.S. *Opt. Laser Technol.*, **35**, 173 (2003).